

DEEP X-RAY OBSERVATIONS OF TWO RADIO MINI-HALOS: TESTING MODELS OF HALO FORMATION

In a search for the most powerful steep¹ spectrum radio sources residing in cool core clusters, we have discovered a pair of rare radio mini-halos (see Figure 1) in the galaxy clusters Abell 2675 ($z = 0.071$) and Zwicky 808 ($z = 0.169$). As a class, mini-halos are characterized by their diffuse, low radio surface brightness, steep radio spectral indices, unilateral association with cool core clusters, confinement of the radio emission to the region of the cluster where ICM cooling times are $\ll H_0^{-1}$, and suspected association with gentle disturbance of the ICM (*e.g.* subsonic mergers). The properties of the extended, resolved radio emission in both clusters are consistent with these criteria: the halo of A2675 has a radius of ≈ 100 kpc, integrated spectral index of ≈ -1.5 , and surface brightness $\mu \approx 50 \mu\text{Jy arcsec}^{-2}$. Likewise, Z808's halo has a radius ≈ 225 kpc, spectral index ≈ -1.4 , and $\mu \approx 700 \mu\text{Jy arcsec}^{-2}$. Further, both clusters are bright X-ray sources detected with *ROSAT* ($L_X > 3 \times 10^{44} \text{ erg s}^{-1}$) and host central dominant (cD) galaxies which are optical line-emitters. The high-X-ray luminosities and close correlation between short central ICM cooling times and line-emitting cDs suggests the clusters both have cool cores, in line with the class of clusters which are known to host mini-halos. A2675 and Z808 are also incredibly rare objects: of the 750 objects in the combined BCS/eBCS/MACS/REFLEX surveys, A2675 and Z808 are two of only 10 clusters that host a line-emitting cD and have an associated steep spectrum radio source with a 74 MHz flux > 1 Jy. Of these 10 objects (the other eight being 2A 0335+096, A133, A496, A2009, A2675, MKW3s, MKW8, MS 0735.6+7421, Z808, Z2701), only A2675 and Z808 have radio morphologies consistent with that of mini-halos.

Why are mini-halos important? The ICM of galaxy clusters is composed of thermal and non-thermal components. The thermal component dominates clusters, and is observed via X-ray bremsstrahlung radiation. Strong evidence exists that halo cooling of clusters with ICM cooling times $< H_0^{-1}$ is regulated primarily by feedback from the cD active galactic nucleus (AGN) [4-6]. At the same time an AGN is influencing the evolution of the thermal component, it also contributes to the non-thermal component by injecting high-energy particles and magnetic fields (\vec{B}) into the host environment. Evidence of this contribution comes from the relativistic jets and synchrotron emission which accompany AGN activity.

Radio mini-halos, like the candidates in A2675 & Z808, may be related to the process of AGN feedback. Interestingly, mini-halos are unilaterally found in clusters with core cooling times < 1 Gyr that host a powerful ($\gtrsim 10^{40} \text{ erg s}^{-1}$) central radio galaxy [7,8]. Unlike high-surface brightness, low-volume FR-I/FR-II sources, mini-halos are characterized by low radio surface brightness ($\sim 1 - 500 \mu\text{Jy arcsec}^{-2}$ at < 400 MHz), large extents which fill the core ($d \lesssim 500$ kpc), and a steep radio spectrum ($\alpha \lesssim -1$). mini-halos ostensibly show no connection to an AGN, and occupy a volume sufficiently large that if the radiating population had originated from a cD AGN, the particles would radiate away their energy prior to reaching the mini-halo outskirts. This strict energetic constraint implies *in situ* particle acceleration, possibly by compressed or shear \vec{B} -fields, or from cosmic-ray ion collisions with the magnetized ICM. However, these explanations are uncertain, and even if they were not, it is unclear where the fields and particles powering mini-halo emission originate and if, like their much larger brethren “giant” and “relic” halos, mini-halos are connected to mergers [9].

Given that $\approx 50\%$ of clusters have cool cores, with $> 90\%$ of them undergoing some level of AGN outburst or minor merger, the number of known mini-halos is curiously small (< 20): 2A 0335+096, A1068, A1413, A1835, A2029, A2052, A2142, A2390, A2626, MRC 0116+111, MS

¹“Steep” spectral index defined using the VLSS & NVSS radio surveys as $\alpha \equiv \log[S(\nu_1)/S(\nu_2)]/\log(\nu_1/\nu_2) < -1.3$, *e.g.* radio sources with substantially more power at decreasing frequency.

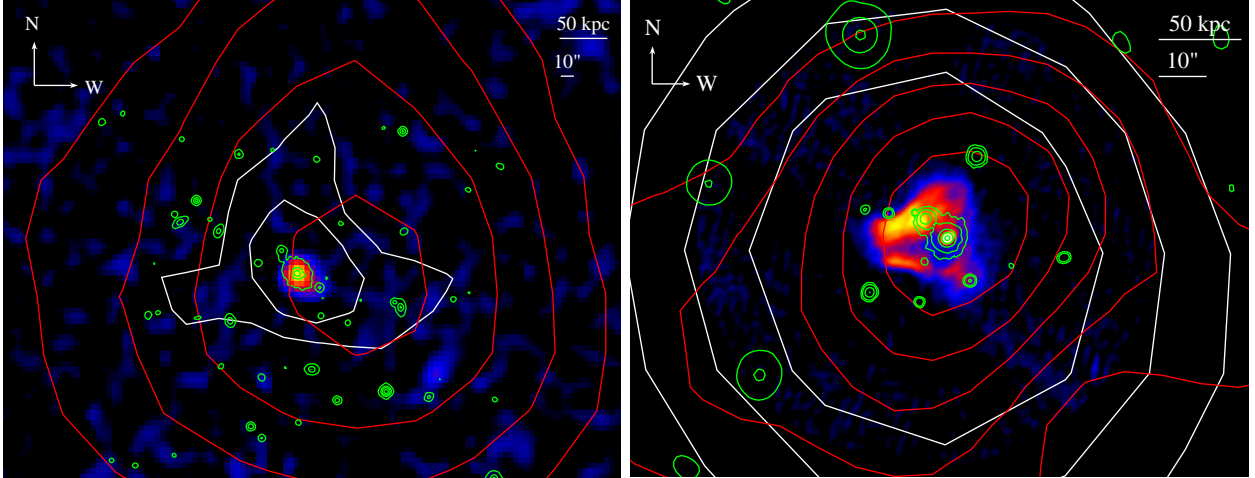


Figure 1: 1.4 GHz VLA radio images of the mini-halo candidates A2675 (*left*) and Z808 (*right*). Red contours are cluster X-ray emission, green contours are optical emission, and white contours are 74 MHz VLA radio emission.

1455.0+2232, Ophiuchus, Perseus, PKS 0745-191, RX J1347.5-1145, and RX J1720.1+2638 [10-18]. We point out that none of these objects simultaneously satisfies all three of the stringent criterion used for selecting our two targets, highlighting that we have identified mini-halo candidates which have the strongest features of other mini-halos. Further, systematic low-frequency searches have yielded few confirmed mini-halos [19,20]. Four mini-halo candidates ($z = 0.3-0.5$) were recently identified with GMRT using a similar NVSS-VLSS radio-selected sample of steep spectrum sources [21]. However, while the GMRT sources are associated with clusters, none of them are detected X-ray sources, giving $L_X \lesssim 4 \times 10^{44} \text{ erg s}^{-1}$. No cD emission lines are detected in three, and there is no spectroscopy for one. So while radio-selected samples exist, their utility in defining candidates for X-ray follow-up is limited.

The paucity of known mini-halos gives credence to the idea that they are highly transient or require very specific ICM conditions to form. While a variety of models have emerged attempting to explain mini-halos [*e.g.* 22-24], the lack of well-studied mini-halo systems inhibits refinement of these models using observational constraints. Additionally, if simulations incorporating AGN feedback are to reproduce the range of non-thermal sources observed in clusters and yield insight to their importance for structure formation & evolution, then better observational constraints must be achieved. To this end, detailed X-ray analysis of mini-halo candidate systems is vital as it enables diagnosis of cluster dynamics (*e.g.* with substructure like cold fronts), AGN energetics (*e.g.* via cavities and shocks), and how these correlate with diffuse non-thermal emission, in ways optical and radio observations are incapable [*e.g.* 25]. Joint high-resolution X-ray and radio study of the ICM in clusters hosting radio halos is required to better understand the link between thermal & non-thermal ICM components and to reveal the physics responsible for particle (re-)acceleration in diffuse radio halos.

ICM cold fronts (CFs) may be an especially useful tool for understanding the connection between a cool core and mini-halo. In some mini-halo models, ICM bulk motions & turbulence are responsible for the re-acceleration of fossil electrons which emit the diffuse synchrotron emission of a mini-halo [*e.g.* 22,24,26]. Interestingly, turbulence and bulk motions (*e.g.* gas sloshing) induced by a subsonic merger event in a dense cluster core are the same processes which excite CFs [27]. A CF is detected as a constant pressure contact discontinuity where downstream gas density and temperature are higher & lower, respectively, than the upstream counterparts. That CFs appear

to be long-lived, in spite of cool, high-density gas being co-spatial with gas sometimes twice as hot, indicates suppression of conduction at the CF face by \vec{B} -fields which are likely draped over the front during its formation [28]. Thus, the properties of a CF (*i.e.* size, thickness, contrast with ambient medium) provide a means for studying cool core \vec{B} -field strengths and configurations. If the \vec{B} -fields which define a CF are the same fields that produce mini-halos, then the study of one illuminates the other. Indeed, there are examples of mini-halo & CFs being present in the same system with indications they are physically related [10,18,29-31]. If more examples like this could be found, a task which requires deep X-ray observations, then the cool core-CF-mini-halo relationship could be explored more thoroughly.

Merger Induced mini-halos in A2675 & Z808? In Fig. 1 note the large companion galaxies within 15 kpc of both cDs and that the radio emission is elongated along the axis including the companions. In both clusters the optical, X-ray, and radio emission are significantly off-set from each other, suggesting the cD is moving relative to the ICM. Also note the peculiar Z808 1.4 GHz morphology: sharp edge to NE of core, hole NW of core, radio plume trailing galaxy SW of cD, compressed “sandwich” appearance. All these features indicate recent merger activity. If so, are there CFs, shocks, or cavities in these systems which would illuminate the connection between the cool core, the mini-halo, and previous AGN feedback? Is the mini-halo power correlated with the cooling luminosity as is expected for models of particle re-acceleration via magnetohydrodynamic (MHD) turbulence? Is there evidence of ICM turbulence in the X-ray emission (*e.g.* eddies or twisted wake like in A520)? Might there be powerful cavities in the X-ray halos of these clusters which can be used to measure the energetics of an AGN outburst and constrain how relativistic plasma is transported in the core? Spurred along by these questions, we propose *Chandra* X-ray observations of 80 ks for A2675 and 100 ks for Z808. We seek to (1) determine if a merger has taken place as evidenced by CFs or shocks, (2) probe for signs of AGN activity like cavities, (3) evaluate the connection of the steep spectrum radio source to the X-ray properties, and (4) model the A2675 & Z808 mini-halos using existing theories to constrain the magnetic field properties and particle content as they relate to the cool core and AGN.

Deep X-ray Data for a Radio Halo? The physics of how mini-halos are formed may be encoded in the X-ray emission of the ICM. The mini-halo model of Gitti et al. (2004) employs MHD turbulence frozen into the gas of the cool core region to re-accelerate fossil electrons. To evaluate the Gitti model requires measurement of core properties derived from X-ray data, specifically the cool core radius (r_c), scaled electron gas density (n_c), and temperature structure (kT_X). The turbulence model of Kunz et al. (2010) and shear model of Keshet et al. (2009) also require these parameters be known. The energy scale where mini-halo synchrotron and inverse Compton (IC) losses are balanced by re-acceleration, γ_b , are related to these quantities by $\gamma_b \propto r_c^{0.8} n_c^{-1}$. If an AGN is responsible for the mini-halos, then the time for radio plasma to reach the edge of the mini-halo should be less than the plasma synchrotron lifetime, t_{sync} . Buoyancy and sound crossing time arguments are useful in constraining the time a plasma takes to move about the ICM [2], and these calculations are based on X-ray measurements ($t_{cs} \propto kT_X^{-1/2}$ and $p \propto n_c kT_X$). Further, constraints on the ICM turbulent energy density, turbulent lengthscale, and diffusion coefficient are required, quantities which are n_c and kT_X dependent. If the cooling luminosity is much larger than the synchrotron power, then at a minimum, cooling flow powered turbulence, P_{CF} , could drive re-acceleration. Since $P_{\text{CF}} \propto \dot{M}$, this can only be constrained using high-SN X-ray spectral analysis of the core. We cannot neglect the possibility that merger shocks have powered the mini-halo. In which case the energy released in the shock, determined from shock morphology and kT_X & n_c dis-

continuities, can be used to constrain the energy spectrum of Fermi accelerated electrons. Because of IC and synchrotron losses, the energy spectrum implies a t_{sync} , which, when set in the context of the mini-halo morphology, determines if the halo could be powered by a shock. We will also measure radial properties of the ICM: gas mass, gravitating mass, entropy, pressure, cooling time, effective conductivity (if a strong $T(r)$ gradient is discovered), and inferred magnetic suppression (to prevent the rapid destruction of a strong $T(r)$ gradient).

Request for Observations: Our time requests are aimed at reaching temperature and density uncertainties necessary for significant detections of a typical CF, weak shock, cavities, and to collect sufficient counts for radial & spatial mapping of ICM structure. Use of ACIS-S versus ACIS-I results in 40-50% more total counts, and the ACIS-S3 FOV encloses a cluster-centric radius of R_{2000} , which is far enough out to probe for large-scale shocks or CFs. Using β -models fitted to the survey *ROSAT* imaging data, Cycle 12 ACIS-S count rates were determined from PIMMS. 5,000 mock surface brightness (MSB) profiles extending to R_{2000} were then generated via a Monte Carlo. Shallow baseline temperature and abundance profiles were also created, $T(r) \propto r^{0.2}$ & $Z(r) \propto r^{-0.2}$, with normalizations $T(R_{2000}) = T_{\text{cluster}}$ & $Z(R_{2000}) = 0.3 Z_{\odot}$. An isothermal core was also used, $T(r < R_{7500}) = T(R_{7500})$. For each MSB profile, cumulative counts profiles were created for exposure times ranging 40-140 ks in 20 ks steps. Bins with 2,500 counts were defined, and mean kT_X and abundance were calculated for each bin from the gradient profiles. A simulated spectrum was generated in XSPEC for each bin using an absorbed thermal model (MEKAL), the corresponding exposure time, and a normalization chosen so the spectral count rate matched the count rate predicted by the MSB profile for that bin. Source images consistent with these parameters were created in IDL, and mock *Chandra* images were created using MARX. A fixed background composed of the PIMMS and RASS R12 & R45 emission was included in all analysis.

Radial profiles were extracted from the simulated data to estimate the mean uncertainties for each exposure time. We find exposure times of 80 ks for A2675 and 100 ks for Z808 return the best uncertainties per unit time while maintaining the highest signal-to-noise such that weighted Voronoi tessellation maps with a minimum binned spatial resolution of $\sim 5\text{--}10''$ can be created. For A2675, the mean uncertainties will be $\Delta T_X \pm 0.3\text{--}0.6$ keV and $\Delta n_c \pm 10\%$, and for Z808, $\Delta T_X \pm 0.5\text{--}0.8$ keV and $\Delta n_c \pm 12\%$. Our simulations indicate we will be sensitive at $> 2\sigma$ to CFs with temperature jumps > 1.5 and density decreases > 1.3 , which are typical values for CFs. Conversely, based on the Rankine-Hugoniot jump conditions, we should detect a $M > 1.2$ shock at $\gtrsim 2\sigma$. We will also be able to measure \vec{B} -field strengths in the CF analysis to $\approx 3\mu\text{G}$, well below the level needed for discerning between mini-halo formation models.

We simulated the presence of cavities in the ICM of our targets by carving out voids in the source images and creating new mock observations with MARX. Cavity decrements, their geometries, and distances from the cluster core span a wide-range of values, thus we placed voids, obeying the radially dependent axial ratio and SB dimming relations presented in [5], at a variety of radii. For spherical plane-of-the-sky cavities, our observations should be sensitive to $> 10\%$ decrements at $r < 100$ kpc and $> 30\%$ decrements at $100 < r < 200$ with no detections expected beyond. Our mock observations loosely indicate we will be sensitive to cavity powers of $10^{41\text{--}46} \text{ erg s}^{-1}$.

(1) Crawford et al. MNRAS 306 857 ‘99; (2) Cavagnolo et al. ApJ 683 L107 ‘08; (3) Ebeling et al. MNRAS 301 881 ‘98; (4) Croton et al. MNRAS 365 11 ‘06; (5) McNamara & Nulsen. ARA&A 45 117 ‘07; (6) Peterson & Fabian. Phys. Rep. 427 1 ‘06; (7) Ferrari et al. Spa. Sci. Rev. 134 93 ‘08; (8) Giovannini et al. A&A 507 1257 ‘09; (9) Feretti & Giovannini. LNP 740 143 ‘08; (10) Baum & O’Dea. MNRAS 250 737 ‘91; (11) Burns et al. ApJ 388 L49 ‘92; (12) Giovannini & Feretti. NewAst 5 335 ‘00; (13) Bacchi et al.

A&A 400 465 ‘03; (14) Gitti et al. A&A 417 1 ‘04; (15) Gitti et al. A&A 470 L25 ‘07; (16) Govoni et al. A&A 499 371 ‘09; (17) Bagchi et al. MNRAS 399 601 ‘09; (18) Mazzotta & Giacintucci. ApJ 675 L9 ‘08; (19) Venturi et al. A&A 463 937 ‘07; (20) Venturi et al. A&A 484 327 ‘08; (21) van Weeren et al. A&A 508 75 ‘09; (22) Gitti et al. A&A 386 456 ‘02; (23) Pfrommer & Enßlin. A&A 413 17 ‘04; (24) Keshet et al; arXiv:0912.3526K, ‘09; (25) Wong et al. ApJ 682 155 ‘08; (26) Kunz et al. arXiv:1003.2719K, ‘10; (27) Ascasibar & Markevitch. ApJ 650 102 ‘06; (28) Markevitch & Vikhlinin. PhyRep 443 1 ‘07; (29) Markevitch et al. ApJ 541 542 ‘00; (30) Zhao et al. ApJ 416 51 ‘93; (31) Mazzotta et al. ApJ 596 190 ‘03.

Previous *Chandra* Programs:

Co-I Edge, GO Cycle 2: “The interaction between radio galaxies and ICM in the cores of clusters.” Observation of two potential cavity systems both of which have been published in larger study of Cavagnolo et al. 2009, ApJS, 182, 12.

Co-I Edge, GO Cycle 4: “Probing the mass profile of clusters to 10 kpc.” Observation of Abell 1201 which has been published in Owers et al. 2009, ApJ, 692, 702.

Co-I McNamara, GO Cycle 8: “AGN Feedback and Galaxy Formation in Cluster Cores.” A study of Abell 1664 by Kirkpatrick et al. 2009, ApJ, 697, 867; a study of RBS 797 is presented in Cavagnolo et al. 2010 (in preparation for ApJ).

Co-I McNamara, GO Cycle 10 LP: “A Deep Image of the Most Powerful Cluster AGN Outburst.” A study of MS 0735.6+7421 utilizing 500 ks of data is underway.

PI Cavagnolo, GO Cycle 10: “The Hyperluminous Infrared Galaxy IRAS 09104+4109: An Extreme Brightest Cluster Galaxy.” A detailed study of IRAS 09104+4109 is presented in Cavagnolo et al. 2010 (in preparation for MNRAS).

PI Cavagnolo maintains the Archive of Chandra Cluster Entropy Profile Tables (ACCEPT) database and is adding 84 galaxy clusters (156 observations) to the 241 clusters currently in the database. As a result of maintaining the database, PI Cavagnolo has reduced & analyzed 752 CXO observations (~ 16 Msec of data) along with over 80,000 spectra.